



## 2 Study of free convective heat transfer from horizontal conic

3 W.M. Lewandowski \*, S. Leble

4 *Department of Apparatus and Chemical Machinery, Gdańsk University of Technology, ul. G. Narutowicza 11/12,*  
5 *80-952 Gdańsk, Poland*

6 Received 16 January 2003; received in revised form 2 April 2003

### 7 Abstract

8 Theoretical and experimental considerations of free convective heat transfer from horizontal isothermal conic in  
9 unlimited space are presented. In the theoretical part of the paper we introduced the curvilinear coordinate system  
10 compatible with conical surface and gravity field. The equations of Navier–Stokes and Fourier–Kirchhoff were sim-  
11 plified in this local orthogonal system. The resulting equation have been solved by asymptotic series in the vicinity of  
12 horizontal element of the cone. The final Nusselt–Rayleigh relation as a function of the conic base angle was verified  
13 experimentally. The experimental study was performed in water and air for conics with the angles equal to  $\alpha = 0$   
14 (vertical round plate),  $30^\circ$ ,  $45^\circ$  and  $60^\circ$  and diameter of the base  $D = 0.1$  m. The experimental results are in a good  
15 accordance (maximum within +8.7%) with the theory.

16 © 2003 Published by Elsevier Ltd.

### 18 1. Introduction

19 The results of theoretical and experimental study of  
20 free convective heat transfer from conical surfaces were  
21 published and they are very useful to determine con-  
22 vective heat losses from conical fragments of apparatus  
23 in industrial or energetic installations, electronic equip-  
24 ment, architectonic objects and so on by engineers and  
25 designers. Unfortunately available dates are not com-  
26 plete. There are some information on vertical faced  
27 down or up cones [1–6] but for the horizontal ones we  
28 have found the only paper, written by Oosthuizen [7]. In  
29 the Churchill's review paper [8] among about 120 results  
30 devoted to free convection four positions are concerned  
31 conical (only vertical) surfaces. Oosthuizen's paper deal  
32 only with the experimental study.

33 Hence the paper presents theoretical solution of the  
34 natural convective heat transfer problem from the iso-  
35 thermal surface of a horizontal conic. We also show the  
36 experimental verification of the obtained analytical for-

37 mulas. The experiments were performed in water and air  
38 for conics with the base angle:  $\alpha = 0^\circ$ ,  $30^\circ$ ,  $45^\circ$  and  $60^\circ$ .

39 The phenomenon of convective fluid flow pattern for  
40 the configuration to be considered is complicated, be-  
41 cause of the gravity field breaks the axis symmetry in  
42 comparison with vertical cones (Fig. 1a). In our first  
43 attempts we used of the cylindrical coordinate system  
44 successive in the case of horizontal cylinder (Fig. 1b) for  
45 the hypoeutectic stream line description (Fig. 1c).  
46 However, more profound study and the visualization  
47 (Fig. 2a) had been shown a failure of this first attempt.

48 This is the reason why we decided to introduce the  
49 special curvilinear coordinate system  $(\epsilon, \epsilon_m)$  based on the  
50 stream line curves  $S_i$ , shown in Fig. 2b and described in  
51 details together with continuous maps, transformations  
52 and final solution in papers [9,10]. We would like to  
53 stress that each curve  $S_i$  is not plain, by other words it is  
54 not conic. The variety of the curves cover the conic  
55 surface and parameterized by  $\epsilon_m = \max(\epsilon)$ .

### 2. The coordinate system and physical model 56

57 The isothermal lateral conic surface in Cartesian  
58 coordinates is described by the equation

\* Corresponding author. Tel.: +48-58-347-24-10; fax: +48-58-347-24-58.

E-mail address: ewarad@chem.pg.gda.pl (W.M. Lewandowski).

**Nomenclature**

$a$  thermal diffusivity ( $\text{m}^2/\text{s}$ )  
 $a$  function defined by Eq. (46)  
 $A$  control surface, Fig. 5 and Eq. (21) ( $\text{m}^2$ )  
 $C$  coefficient in Nusselt–Rayleigh relation Eq. (30) (dimensionless)  
 $c_p$  specific heat at constant pressure ( $\text{J}/(\text{kg K})$ )  
 $D$  diameter of the cone base (m)  
 $dA_k$  control surface of heated wall, Fig. 5 and Eq. (22) ( $\text{m}^2$ )  
 $E$  coefficient in Eq. (31)  
 $f = y''(0)$  coefficient in the Taylor expansion of  $y(\epsilon)$   
 $F$  coefficient in Eq. (31)  
 $g$  acceleration due to gravity ( $\text{m}/\text{s}^2$ )  
 $g = y'(0)$  coefficient in the Taylor expansion of  $y(\epsilon)$   
 $G$  coefficient in Eq. (31)  
 $h$  heat transfer coefficient ( $\text{W}/(\text{m}^2 \text{K})$ )  
 $H$  length of the horizontal conic (m)  
 $H$  coefficient in Eq. (31)  
 $I$  current of the heater (A)  
 $J$  constant defined by integral (52) (dimensionless)  
 $K$  constant in the relation (26) (dimensionless)  
 $Nu = \frac{hR}{\lambda}$ ,  $= \frac{hD}{\lambda}$  Nusselt number (dimensionless)  
 $M$  arbitrary point of the conical surface  
 $p$  pressure ( $\text{N}/\text{m}^2$ )  
 $P$  function defined by Eq. (46)  
 $r = \rho_0 K^{1/3}$  dimensionless radius coordinate (dimensionless)  
 $R$  radius of the cone (m)  
 $Q$  heat flow (W)  
 $Ra = \frac{g\beta\Delta T R^3}{\nu\alpha}$ ,  $= \frac{g\beta\Delta T D^3}{\nu\alpha}$  Rayleigh number (dimensionless)  
 $s$  unit vector, tangent to the curve  $S$  (dimensionless)

$S$  curve, being the convective fluid flow streamlines on the lateral surface of the horizontal conic (dimensionless)  
 $T$  temperature ( $^\circ\text{C}$ ) or (K)  
 $T_w$  wall temperature ( $^\circ\text{C}$ )  
 $T_\infty$  bulk fluid temperature ( $^\circ\text{C}$ )  
 $\Delta T$  temperature difference (K)  
 $U$  voltage of the heater (V)  
 $W$  velocity (m/s)  
 $x$  coordinate (m)  
 $X_i$  constants in Eqs. (27)–(30) (dimensionless)  
 $y(\epsilon)$  dimensionless boundary layer thickness (dimensionless)  
 $y$  coordinate (m)  
 $Y = y(0)$  coefficient in the Taylor expansion of  $y(\epsilon)$   
 $z$  coordinate (m)  
 $Z = Y^4$  function of the  $Y$  (dimensionless)

*Greek symbols*

$\alpha$  base angle of the conic (deg)  
 $\beta$  average volumetric thermal expansion coefficient ( $1/\text{K}$ )  
 $\delta$  boundary layer thickness (m)  
 $\epsilon$  angle defined in Fig. 2 (deg)  
 $\zeta$  distance between curves  $S$  (Fig. 5) (m)  
 $\lambda$  thermal conductivity of the fluid ( $\text{W}/(\text{m K})$ )  
 $\nu$  kinematic viscosity ( $\text{m}^2/\text{s}$ )  
 $\rho$  radius defined in Fig. 3 (m)  
 $\rho_f$  density of the fluid ( $\text{kg}/\text{m}^3$ )  
 $\sigma$  vector normal to the curve  $S$  (m)  
 $\tau$  vector tangent to the curve  $S$  (m)  
 $\Theta$  nondimensional temperature [–]  
 $\Sigma$  lateral surface of the conic

$$x^2 + y^2 - z^2 \cot^2(\alpha) = 0, \quad 0 \leq z \leq H \quad (1)$$

60 or by  $\rho$ ,  $\epsilon$ ,  $z$ , where  $x = \rho \sin(\epsilon)$ ,  $y = \rho \cos(\epsilon)$  (Fig. 3). The  
 61 base angle  $\alpha$  is a parameter of the conical surface which  
 62 varied from  $\alpha = \pi/2$ —horizontal cylinder to  $\alpha = 0$ —  
 63 round vertical plate.

64 At arbitrary point  $M_i$  of the lateral conical surface  $\Sigma$   
 65 one may distinguish two tangent vectors  $\bar{\tau}_\rho$  and  $\bar{\tau}_\epsilon$  and  
 66 normal  $\bar{\sigma}$  to the surface.

$$\bar{\tau}_\rho = \frac{\partial \bar{r}}{\partial \rho}, \quad \bar{\tau}_\epsilon = \frac{\partial \bar{r}}{\partial \epsilon} \quad \text{where } \bar{r} = (x, y, z) \in \Sigma, \quad (2)$$

$$\bar{\sigma} = \bar{i} \sin \alpha \sin \epsilon + \bar{j} \sin \alpha \cos \epsilon - \bar{k} \cos \alpha. \quad (3)$$

9 Decomposition of the gravity with respect to these  
 0 coordinates gives the normal component of gravity force  
 1  $g_\sigma = g \sin \alpha \sin \epsilon$ ,  $\bar{g} = (-g, 0, 0) = -\bar{i}g$ .

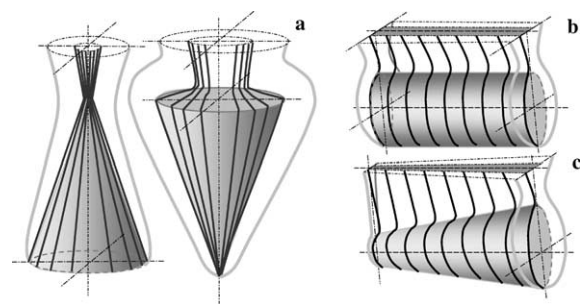
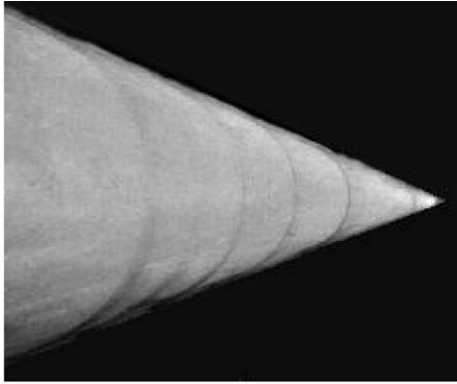
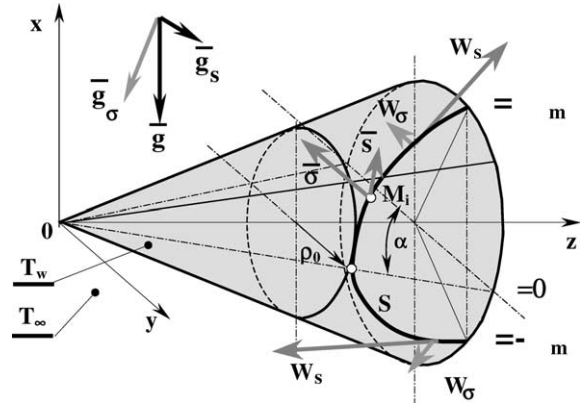


Fig. 1. Free convective fluid flow pattern described by boundary layer thickness (black lines) and stream lines close heated surface and in a plume (gray lines) for: (a) vertical cones, (b) horizontal cylinder and (c) horizontal conic.



a



b

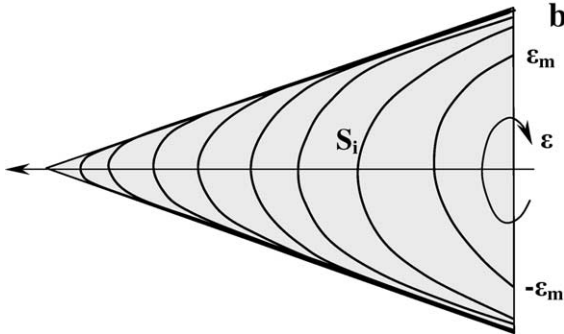


Fig. 2. Result of the visualization of the stream lines on the horizontal, isothermal conic transferred heat by free convection (a) and the model of the phenomenon described by curvilinear coordinate system  $(\epsilon, l)$  with stream line curves  $S_i$  (b).

Let us now define a tangent component of the gravity. After normalization this component takes the form

$$\bar{s} = \frac{\bar{g} - (\bar{g}, \bar{\sigma})\bar{\sigma}}{g\sqrt{1 - \sin^2 \alpha \sin^2 \epsilon}} = \frac{-\bar{i}(1 - \sin^2 \alpha \sin^2 \epsilon) + \bar{j} \sin^2 \alpha \sin \epsilon \cos \epsilon - \bar{k} \cos \alpha \sin \alpha \sin \epsilon}{\sqrt{1 - \sin^2 \alpha \sin^2 \epsilon}} \quad (4)$$

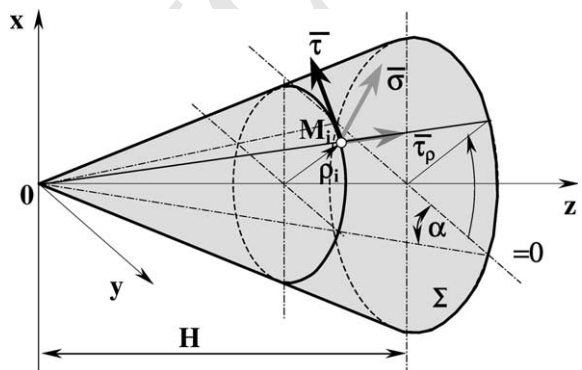


Fig. 3. Coordinate systems: Cartesian, curvilinear and local for the conic.

Fig. 4. The illustration of the curve  $S$  construction: it is defined as the vector  $\bar{s}$  is tangent at every point of the curve  $S$ .

This unit vector  $\bar{s}$  defines the curve  $S$  on the surface (Fig. 4). Hence the gravity component along  $\bar{s} \times \bar{\sigma}$  is zero. That is why we solve the equations: Navier–Stokes, Fourier–Kirchhoff and continuity in these two characteristic directions  $\bar{\sigma}$  and  $\bar{s}$ .

We use assumptions typical for natural convection [9]:

- fluid is incompressible and its flow is laminar, 81
- inertia forces are negligibly small in comparison with viscosity ones, 82 83
- the mass density  $\rho_f$ , kinematic viscosity  $\nu$  and volumetric expansion  $\beta$  in the boundary layer and undisturbed region (index  $\infty$ ) are constant, 84 85 86
- tangent to the heated surface component of the velocity inside the boundary layer is significantly larger than normal one  $W_s \gg W_\sigma$ . By this assumption two marginal regions are excluded: the first where the boundary layer arises  $\epsilon = -\epsilon_m$  and the second where it is transferred into the free buoyant plume  $\epsilon = \epsilon_m$ . 87 88 89 90 91 92
- temperature of the lateral conical surface  $T_w$  is constant, 93 94
- thicknesses of the thermal and hydraulic boundary layers are the same. 95 96

Finally the Navier–Stokes equations may be written 97

$$\nu \frac{\partial^2 W_s}{\partial \sigma^2} - g_s \beta (T - T_\infty) - \frac{1}{\rho_f} \frac{\partial p}{\partial s} = 0, \quad (5)$$

$$-g_\sigma \beta (T - T_\infty) - \frac{1}{\rho_f} \frac{\partial p}{\partial \sigma} = 0. \quad (6)$$

The coordinates  $\sigma$  and  $s$  are local ones along the vectors  $\bar{\sigma}$  and  $\bar{s}$ . 100 101

We evaluate the normal and tangent components of gravity as 102 103

$$g_\sigma = \bar{\sigma} \cdot \bar{g} = -g \sin \alpha \sin \epsilon, \quad (7)$$

$$g_s = g \sqrt{1 - \sin^2 \alpha \sin^2 \epsilon}. \quad (8)$$

106 We assumed that relation for temperature distribu-  
107 tion inside boundary layer can be used as solution of  
108 Fourier–Kirchhoff equation [10,11]

$$\Theta = \frac{T - T_\infty}{T_w - T_\infty} = \left(1 - \frac{\sigma}{\delta}\right)^2 \quad \text{or} \quad T - T_\infty = \Delta T \left(1 - \frac{\sigma}{\delta}\right)^2. \quad (9)$$

110 Plugging (7)–(9) into (5) and (6) gives

$$v \frac{\partial^2 W_s}{\partial \sigma^2} - g\beta\Delta T \left(1 - \frac{\sigma}{\delta}\right)^2 \sqrt{1 - \sin^2 \alpha} \sin \epsilon - \frac{1}{\rho_f} \frac{\partial p}{\partial s} = 0. \quad (10)$$

$$-g\beta\Delta T \sin \alpha \sin \epsilon \left(1 - \frac{\sigma}{\delta}\right)^2 - \frac{1}{\rho_f} \frac{\partial p}{\partial \sigma} = 0. \quad (11)$$

113 Integration of Eq. (11) for the boundary condition  
114  $\sigma = \delta$ ,  $p_\sigma = p_{\infty(\sigma \geq \delta)}$  gives a formula for the pressure  
115 distribution in a boundary layer directed tangent to the  
116 heating surface.

$$p_\sigma = -p_{\infty(\sigma \geq \delta)} - \rho_f g \beta \Delta T \sin \alpha \sin \epsilon \left( \sigma - \frac{\sigma^2}{\delta} + \frac{\sigma^3}{3\delta^2} - \frac{\delta}{3} \right). \quad (12)$$

118 Pressure  $p_{\infty(\sigma \geq \delta)}$  represents the excess of pressure  
119 over the hydrostatic pressure, on the border of the  
120 boundary layer, which, as it was shown in the paper [11],  
121 is approximately constant.

122 Differentiating of Eq. (12) with respect to  $s$  along the  
123 curve  $S$  (for the complete derivation of the curve equation  
124 look [9]), parameterized by the minimum value  $\rho_0$  of  $\rho$

$$\rho = \rho_0 (\cos \epsilon)^{-\cos^2 \alpha} \quad (13)$$

126 gives

$$\frac{\partial p}{\partial s} = -\rho_f g \beta \Delta T \sin \alpha \frac{(\cos \epsilon)^{\cos^2 \alpha + 1}}{\rho_0 \sqrt{1 - \sin^2 \epsilon} \sin^2 \alpha} \left[ \cos \epsilon \left( \sigma - \frac{\sigma^2}{\delta} + \frac{\sigma^3}{3\delta^2} - \frac{\delta}{3} \right) + \sin \epsilon \left( \frac{\sigma^2}{\delta} - \frac{2\sigma^3}{3\delta^3} - \frac{1}{3} \right) \frac{d\delta}{d\epsilon} \right]. \quad (14)$$

128 The parametrization of the curve  $S$  by  $\rho_0$  in (13) is  
129 equivalent to the parametrization by

$$\epsilon_m = \arcsin \rho_0 / R - \pi/2. \quad (15)$$

131 Plugging of the equality (14) into Eq. (10) leads to

$$v \frac{\partial^2 W_s}{\partial \sigma^2} + \rho_f g \beta \Delta T \left\{ - \left(1 - \frac{\sigma}{\delta}\right)^2 \sqrt{1 - \sin^2 \alpha} \sin \epsilon + \frac{\sin \alpha (\cos \epsilon)^{\cos^2 \alpha + 1} \cos \epsilon}{\rho_0 \sqrt{1 - \sin^2(\epsilon)} \sin^2(\alpha)} \left( \sigma - \frac{\sigma^2}{\delta} + \frac{\sigma^3}{3\delta^2} - \frac{\delta}{3} \right) + \sin \epsilon \left( \frac{\sigma^2}{\delta} - \frac{2\sigma^3}{3\delta^3} - \frac{1}{3} \right) \frac{d\delta}{d\epsilon} \right\} = 0. \quad (16)$$

A double integration of Eq. (16) for the boundary  
conditions  $W_s = 0$  at  $\sigma = 0, \delta$  and mean value evaluation  
through boundary layer gives:

$$\begin{aligned} \bar{W}_s &= \frac{1}{\delta} \int_0^\delta W_s d\sigma \\ &= \frac{g\beta\Delta T \delta^2 (\cos \epsilon)^{\cos^2 \alpha + 1}}{v \sqrt{1 - \sin^2 \epsilon} \sin^2 \alpha} \left( -\frac{1 - \sin^2 \epsilon \sin^2 \alpha}{40 (\cos \epsilon)^{\cos^2 \alpha + 1}} \right. \\ &\quad \left. + \frac{\sin \alpha \cos \epsilon \delta}{180 \rho_0} + \frac{\sin \alpha \sin \epsilon}{72 \rho_0} \frac{d\delta}{d\epsilon} \right) \end{aligned} \quad (17)$$

The account the law of energy conservation

$$dQ = -\rho_f c_p (T - T_\infty) d(A \bar{W}_s), \quad (18)$$

where  $A$  is the cross-section area of the boundary layer  
(see Fig. 5), after the substitution of the mean value of  
the temperature:  $(T - T_\infty) = \frac{\Delta T}{3}$  yields:

$$dQ = -\frac{1}{3} \rho_f c_p \Delta T d(A \bar{W}_s). \quad (19)$$

The heat flux described by Eq. (19) should be equal  
to the heat flux determined by the Newton's equation  
(20):

$$dQ = -\lambda \left( \frac{\partial \Theta}{\partial \sigma} \right)_{\sigma=0} \Delta T dA_k, \quad (20)$$

where  $dA_k$  is the control surface of the conic (see Fig. 5).

The simplifying assumption of the temperature pro-  
file inside boundary layer (9), the dimensionless tem-  
perature gradient on the heated surface may be  
evaluated as

$$\left( \frac{\partial \Theta}{\partial \sigma} \right)_{\sigma=0} = -\frac{2}{\delta}$$

leads to

153

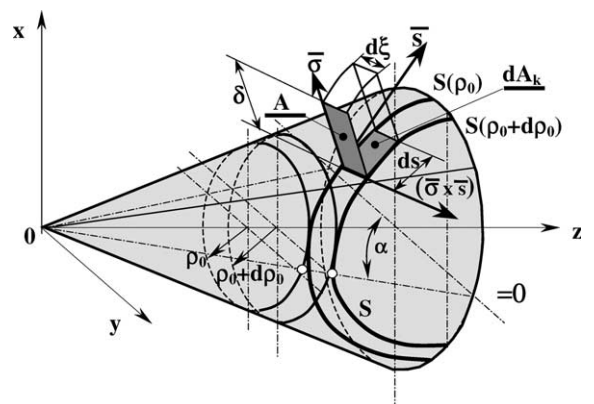


Fig. 5. Presentation of the elementary control surfaces:  $A$  and  $dA_k$ , defined by Eq. (21) and (22) for the coordinate curves  $S(\rho_0)$  and  $S(\rho_0 + d\rho_0)$  and the distance  $d\xi$  between them.

$$\frac{1}{6\lambda} \rho_f c_p \delta d(A\overline{W}_\tau) = -dA_k. \quad (21)$$

155 The definitions of the cross-sectional area and the control  
156 surface  $A$  and  $dA_k$  are:

$$A = d\xi\delta = \frac{-(\cos\epsilon)^{1-\cos^2\alpha} d\rho_0\delta}{\cos\alpha\sqrt{1-\sin^2\alpha\sin^2\epsilon}}, \quad (22)$$

$$dA_k = d\xi d\tau = \frac{-(\cos\epsilon)^{-2\cos^2\alpha} \rho_0 d\epsilon d\rho_0}{\cos\alpha}, \quad (23)$$

159 where

$$d\xi = \left| [\vec{\sigma} \times \vec{\tau}] d\vec{r} \right| = \frac{-(\cos\epsilon)^{1-\cos^2\alpha} d\rho_0}{\cos\alpha\sqrt{1-\sin^2\alpha\sin^2\epsilon}}, \quad (24)$$

161 Substituting Eqs. (17), (22) and (23) in Eq. (21) and  
162 evaluating the differentials one have

$$X_3(\delta\delta'' + 3\delta'^2) + (4X_2 + X_3')\delta\delta' + X_2'\delta^2 + 3X_1\rho_0\delta' + X_1'\rho_0\delta = \frac{\rho_0^2 X_4}{K\delta^3}, \quad (25)$$

164 where

$$K = \frac{Ra_R}{240R^3} = \frac{\rho_f c_p}{240\lambda} \frac{g\beta\Delta T}{\nu}, \quad Ra_R = \frac{g\beta\Delta TR^3}{\nu\alpha} \quad (26)$$

$$X_1 = -(\cos\epsilon)^{1-\cos^2\alpha}, \quad (27)$$

$$X_2 = \frac{2(\cos\epsilon)^{3+\cos^2\alpha} \sin\alpha}{9(1-\sin^2\alpha\sin^2\epsilon)}, \quad (28)$$

$$X_3 = \frac{5(\cos\epsilon)^{2+\cos^2\alpha} \sin\alpha \sin\epsilon}{9(1-\sin^2\alpha\sin^2\epsilon)}, \quad (29)$$

$$X_4 = (\cos\epsilon)^{-2\cos^2\alpha}. \quad (30)$$

170 Eq. (25) is the nonlinear ordinary differential equation  
171 to be considered as the basic one for free convection  
172 heat transfer along the arbitrary curve  $S$  which family  
173 covers the whole surface of isothermal horizontal conic.

### 174 3. Analytical approximate solution of the resulting equation

175 The resulting equation of the physical model could be  
176 solved by a simple numerical method. We, however,  
177 would apply analytical method to construct approximate  
formulas for the boundary layer thickness  $\delta$  as a function  
of variables  $\epsilon$  and  $\rho_0$ . Let us underline that our choice of  
the coordinate system allows to consider  $\rho_0$  as a parameter.  
Rescaling in (25)  $y(\epsilon) = \delta K^{1/3}$ ,  $r = \rho_0 K^{1/3}$  yields:

$$y^4(\epsilon)E \frac{\partial y(\epsilon)}{\partial \epsilon} + 3y^3(\epsilon)E \frac{\partial y(\epsilon)^2}{\partial \epsilon} + y^3(\epsilon) \frac{\partial y(\epsilon)}{\partial \epsilon} G + y^5(\epsilon)H + y^4(\epsilon)F = r^2(1-\sin^2\alpha\sin^2\epsilon)\cos^{-2\cos^2\alpha}\epsilon. \quad (31)$$

where the coefficients are defined by

183

$$E = X_3(1-\sin^2\alpha\sin^2\epsilon) = \frac{5}{9}\cos^{2+\cos^2\alpha}\epsilon\sin\alpha\sin\epsilon, \quad (32)$$

$$G = [y(4X_2 + X_3') + 3X_1r](1-\sin^2\alpha\sin^2\epsilon) = 3(\cos^{1-\cos^2\alpha}\epsilon)r(\cos^2\epsilon + \cos^2\alpha - \cos^2\epsilon\cos^2\alpha) + \frac{8}{9}(\cos^{3+\cos^2\alpha}\epsilon\sin\alpha)y(\epsilon), \quad (33)$$

$$H = X_2'(1-\sin^2\alpha\sin^2\epsilon) = \frac{2}{9}\frac{\sin\epsilon\sin\alpha}{\sin^2\alpha\sin^2\epsilon-1}\cos^{2+\cos^2\alpha}\epsilon(\sin^2\epsilon\cos^4\alpha + 3\cos^2\alpha + \cos^2\epsilon), \quad (34)$$

$$F = X_1'r(1-\sin^2\alpha\sin^2\epsilon) = \frac{r\sin^2\alpha(1-\sin^2\alpha\sin^2\epsilon)}{\cos\cos^2\alpha}\sin\epsilon. \quad (35)$$

We consider an asymptotic solution as a power series in the vicinity of the point  $\epsilon = 0$ . This point is the singularity point of the equation: the coefficient by the second derivative is equal to zero when  $\epsilon = 0$ . The formal Taylor series expansion is

188  
189  
190  
191  
192

$$y(\epsilon) = \sum_{i=0}^{\infty} c_i \epsilon^i = Y + g\epsilon + f\epsilon^2/2 + \dots$$

The coefficients of the expansion we determine directly from the differential equation (31) in the point  $\epsilon = 0$ . The equation gives connection of all coefficients with the first one  $Y = y(0)$ . This unique parameter is defined via the boundary condition  $y(\epsilon_m) = 0$  in the point  $\epsilon = \epsilon_m = \arccos(\rho_0/R)$ .

194  
195  
196  
197  
198  
199

Let us evaluate the first derivative of  $y(\epsilon)$  at the point ( $\epsilon = 0$ ). We start from Eq. (31) and solve it with respect to:

200  
201

$$g = \left[ \frac{\partial y(\epsilon)}{\partial \epsilon} \right]_{\epsilon=0} = \frac{9r^2}{(27r + 8(\sin\alpha)Y)Y^3}. \quad (36)$$

Next we should evaluate the second derivative of  $y(\epsilon)$  at the point  $\epsilon = 0$ . For this aim we differentiate Eq. (36) and then solve the result with respect to:

203  
204  
205

$$f = \left[ \frac{\partial^2 y(\epsilon)}{\partial \epsilon^2} \right]_{\epsilon=0} = -9 \frac{423r^4(\sin\alpha)Y + 729r^2(r^3 + rY^8\sin^2\alpha + (\sin\alpha)Y^9)}{Y^7(27r + 13(\sin\alpha)Y)(27r + 8(\sin\alpha)Y)^2} - 9 \frac{16Y^9(\sin^2\alpha)(Y + r\sin\alpha)(4(\sin\alpha)Y + 27r)}{Y^7(27r + 13(\sin\alpha)Y)(27r + 8(\sin\alpha)Y)^2}. \quad (37)$$

Details of the derivation of (36) and (37) are shown in papers [9,10].

207  
208

Now we introduce the boundary condition at the edge of the cone, where the boundary layer arises

209  
210

$$y(-\epsilon_m) = 0. \quad (38)$$

212 Here we restrict ourselves by parabolic approxima-  
213 tion for the asymptotic expansion of the solution  $y$  of the  
214 differential equation of the boundary layer (31) in the  
215 form

$$y(\epsilon) = Y + g\epsilon + \frac{1}{2}f\epsilon^2. \quad (39)$$

217 Eq. (38) for the parameter  $Y$  is algebraic equation of  
218 high order, which has no explicit solution. So we expand  
219 the equation in Taylor series with respect to the variable  
220  $z = Y \sin \alpha/r$ . In the region  $(1/2)Y \sin \alpha \ll r$  one have in  
221 the first approximation

$$g = \frac{1}{3} \frac{r}{Y^3}, \quad (40)$$

$$f = -\frac{1}{3} \frac{r^2}{Y^3}. \quad (41)$$

224 After substitution of (40) and (41) into Eq. (39) it  
225 simplifies

$$Y^8 - \frac{1}{3} r \arccos(\rho_0/R) Y^4 - \frac{1}{6} r^2 \arccos^2(\rho_0/R) = 0. \quad (42)$$

227 Introducing the new variable  $Z = Y^4$  one goes to the  
228 second-order equation  $Z^2 - (1/3)r \arccos(\rho_0/R)Z -$   
229  $(1/6)r^2 \arccos^2(\rho_0/R) = 0$ .

230 Solution has two roots, the first one is negative, hence  
231 non-physical and the second is positive, hence

$$Y = Z^{1/4} = \sqrt[4]{\frac{1}{2} \left( \frac{1}{6} + \frac{1}{6} \sqrt{7} \right) r [\pi - 2 \arcsin(\rho_0/R)]}. \quad (43)$$

233 Finally the boundary layer thickness is

$$\delta(\epsilon) = \left( \frac{240 \rho_0 R^3}{Ra} \right)^{1/4} \left( \sqrt[4]{\frac{1}{12} (1 + \sqrt{7}) [\pi - 2 \arcsin(\rho_0/R)]} + \frac{\epsilon}{3 \left( \frac{1}{12} (1 + \sqrt{7}) [\pi - 2 \arcsin(\rho_0/R)] \right)^{3/4}} - \frac{\epsilon^2}{6 \left( \frac{1}{12} (1 + \sqrt{7}) [\pi - 2 \arcsin(\rho_0/R)] \right)^{7/4}} \right). \quad (44)$$

#### 236 4. Integral heat transfer coefficient for practical applica- 237 tions

8 The solution (44) is local. However for practical ap-  
9 plications one use the mean value of heat transfer co-  
0 efficient, that is defined as the integral of the local value  
1 over the whole body surface.

2 From Eq. (20) it follows that the local value of heat  
3 transfer coefficient is

$$h = \frac{2\lambda}{\delta}. \quad (45)$$

The expression for boundary layer thickness (44) may be  
rewritten as

$$\delta(\epsilon) = R \left( \frac{240 (\cos \epsilon_m)}{Ra} \right)^{1/4} a(\epsilon_m) \cdot P \left( \frac{\epsilon}{\epsilon_m} \right), \quad (46)$$

where 248

$$a(\epsilon_m) = \sqrt[4]{\frac{1}{6} (1 + \sqrt{7})} \epsilon_m,$$

$$P \left( \frac{\epsilon}{\epsilon_m} \right) = 1 + \frac{\epsilon}{\frac{1}{2} (1 + \sqrt{7}) \epsilon_m} - \frac{\epsilon^2}{\frac{1}{6} (1 + \sqrt{7})^2 \epsilon_m^2} = \left( 1 + \frac{\epsilon}{3a^4} - \frac{\epsilon^2}{6a^8} \right).$$

251 Taking into account above given transformations of  
252 boundary layer thickness the local heat transfer coeffi-  
253 cient  $h$  and it's dimensionless form  $Nu$  are:

$$Nu = \frac{h \cdot R}{\lambda} = \frac{2}{(\cos \epsilon_m)^{1/4} a(\epsilon_m) P \left( \frac{\epsilon}{\epsilon_m} \right)} \left( \frac{Ra}{240} \right)^{1/4}. \quad (47)$$

255 The mean value of Nusselt number for whole lateral  
256 surface of horizontal conic  $S$  can be expressed by the  
257

$$Nu_m = \frac{2}{S} \left( \frac{Ra}{240} \right)^{1/4} \int_0^{\pi/2} \int_{-\epsilon_m}^{\epsilon_m} \frac{1}{(\cos \epsilon_m)^{1/4} a(\epsilon_m) P \left( \frac{\epsilon}{\epsilon_m} \right)} \cdot dA_k. \quad (48)$$

259 Control surface of the cone  $dA_k$  is described with the  
260 use of  $\rho_0$  (13) and  $d\rho_0$  as the functions of  $\epsilon_m$  (15):

$$dA_k = \cos \alpha \cdot (\cos \epsilon)^{-2 \cos^2 \alpha} \cdot R^2 \cdot \sin \epsilon_m \cdot (\cos \epsilon_m)^{2 \cos^2 \alpha - 1} d\epsilon_m d\epsilon. \quad (49)$$

262 Plugging (49) into (48) leads to final relation

$$Nu_m = C_R \cdot Ra^{1/4}, \quad (50)$$

where 264

$$C_R = \frac{2}{\pi} (\cos \alpha)^2 \left( \frac{1}{240} \right)^{1/4} J \quad (51)$$

and 266

$$J = \int_0^{\pi/2} \left( \frac{\sin \epsilon_m (\cos \epsilon_m)^{2 \cos^2 \alpha - 1}}{(\cos \epsilon_m)^{1/4} a(\epsilon_m)} \right) \times \left( \int_{-\epsilon_m}^{\epsilon_m} \frac{(\cos \epsilon)^{-2 \cos^2 \alpha} d\epsilon}{P \left( \frac{\epsilon}{\epsilon_m} \right)} \right) d\epsilon_m. \quad (52)$$

268 For practical application the obtained solution re-  
269 quires evaluation of the double integral over the surface  
270  $J$  (52) which we made numerically. These calculations  
271 were performed for the following numbers of integration

272 steps:  $n = 300$ , for the internal integral and  $p = 150$ , for  
 273 the external one. The model of the boundary layer (44) is  
 274 simplified, the direct corollary of this is the deviation of  
 275 the asymptotic behavior of the local Nusselt number at  
 276 the vicinity of the point  $-\epsilon_m$ , where the boundary layer  
 277 arises. The integral (52) is hence divergent in this point.  
 278 To regularize this discrepancy we integrate from the  
 279 starting step  $-147$  in all calculations. The results of the  
 280 integral evaluations are:  $J = 7.9359, 10.337, 14.885$  and  
 281  $25.692$  for  $\alpha = 0, 30^\circ, 45^\circ$  and  $60^\circ$ , respectively, and next:  
 282  $C_R = 0.6478, 0.6270, 0.6019$  and  $0.5194$  for  $\alpha = 0, 30, 45$   
 283 and  $60$  degrees for the radius of the cone base  $R$  as a  
 284 characteristic linear dimension in Nusselt-Rayleigh rela-  
 285 tion (47) and (26). For comparison with experimental  
 286 results elaborated with the use of the diameter  $D = 2R$  as  
 287 the characteristic linear dimension one can obtain:  
 288  $C_D = \sqrt[3]{2} \cdot C_R = 0.763, 0.746, 0.716$  and  $0.618$  for  $\alpha = 0,$   
 289  $30^\circ, 45^\circ$  and  $60^\circ$  respectively.

## 290 5. Experimental apparatus

291 The experimental studies were performed in two set-  
 292 ups using two fluids: distilled water and air. The both  
 293 set-ups consist of a Plexiglas tank in a form of a rect-  
 294 angular prism of the volume  $150 \text{ dm}^3$  for the water as a  
 295 test fluid and  $200 \text{ dm}^3$  for the air. The visualization of  
 296 convective flow structures was performed in the water  
 297 only while the quantitative experiments were made both  
 298 in the water and in the air for four cones:  $\alpha = 0$  (vertical  
 299 round plate),  $\pi/6, \pi/4$  and  $\pi/3$ . The investigated sam-  
 300 ples, excluding the vertical round plate ( $\alpha = 0$ ), consist  
 301 of two identical copper cones of the base diameter  
 302  $D = 0.1 \text{ m}$ , that were joined in pairs according with Fig.  
 303 6 by the epoxy-resin (DISTAL). Each cone couple was  
 304 suspended in a horizontal position by the use of nylon  
 305 fishing twine of the diameter  $0.1 \text{ mm}$ . In this way the heat  
 306 losses through the base or supports were eliminated. We  
 307 assumed that the heat losses through electric wiring were  
 308 negligible small. The electric resistor as a source of heat  
 309 was placed symmetrically inside the cavity of each  
 310 sample. The concept of performed experimental mea-  
 311 surement of a convective heat flux and the construction  
 312 of the round vertical plate of the diameter  $D = 0.07 \text{ m}$   
 313 were different in comparison with the cone case. The  
 314 vertical plate of the sandwich layer construction con-  
 sisted of two circular copper plates and epoxy-resin  
 circular plate, of known thickness and heat conduction  
 coefficient, between them was used in experiments. In  
 this case the back heat losses flux was measured inde-  
 pendently from temperature differences on both sides of  
 epoxide plate with respect to Fourier equation. The  
 thermal coefficient of conductivity for the laminate  
 (copper-epoxy-resin-copper) was experimentally deter-  
 mined at a specially constructed stand. More details for  
 this case one can found in our previous paper [14].

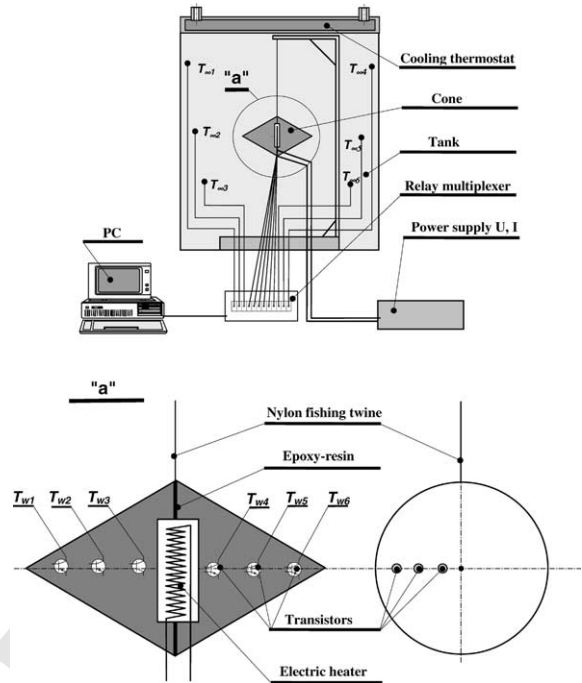


Fig. 6. Arrangement of the experimental apparatus and tested conic (enlarged detail "a").

The surface of the cones were polished and next covered by chromium (electroplating) because the radiative heat losses have to be also taken into account in the experiments performed in the air. In calculations the emissive coefficient for the polished chromium was taken from the physical constants tables.

At the top of the tanks a cooler with thermostatic water of temperature equal to surrounding  $\pm 0.1 \text{ K}$  was mounted. To measure the surface temperature  $T_w$  of the cones six transistors of the type BL 8473 were used. The transistors inserted through the opening of diameter  $1 \text{ mm}$  drilled from the base were glued by epoxy-resin to the surface of the cone. Also six transistors measured the fluid temperature in the undisturbed region  $T_\infty$ . The temperatures of cone surfaces and fluids were calculated as a average value of all the particular transistors  $T_{w,i}$  and  $T_{\infty,i}$ . The output signals from the transistors were processed by a computer program.

Experimental determination of Nusselt number was accomplished with an accuracy of  $\pm 6.6\%$  for the water and  $\pm 5.6\%$  for the air. The accuracy of Rayleigh numbers evaluation were  $\pm 4.3\%$  (water) and  $\pm 2.1\%$  (air).

## 6. Experimental results

Experimental results obtained for the water (dark points) and the air (white points) for the cones of the

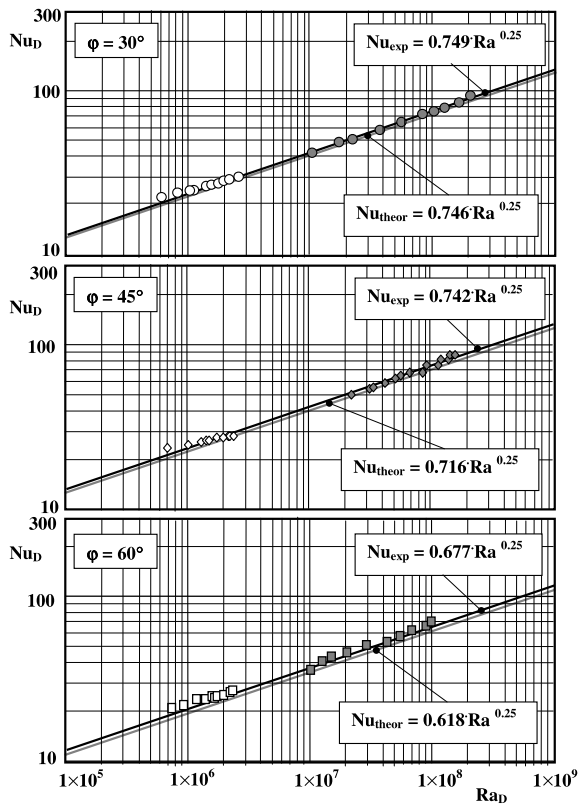


Fig. 7. Comparison of the theoretical results (brown lines) with the experiments (black line) performed in the air (white points) and the water (dark points).

base angle  $\alpha = 30^\circ, 45^\circ$  and  $60^\circ$  and analytical solution (grey lines) are presented in Fig. 7. By using the least square method the experimental data have been correlated by Nusselt–Rayleigh relation  $Nu_D = C \cdot Ra_D^n$  for given value of the exponent  $n = 1/4$ . The results of these approximations together with the present solutions and literature data have been shown in Table 1. and in the frames in Fig. 7.

The Nusselt–Rayleigh formulas in Table 1 are valid for the range of the performed experimental studies:  $6 \times 10^5 < Ra < 2 \times 10^8$  for air and  $1 \times 10^7 < Ra < 2 \times 10^8$  for water which was obtained at wall-to-liquid temperature differences  $9 \text{ K} \leq \Delta T \leq 43 \text{ K}$  for air and  $0.7 \text{ K} \leq \Delta T \leq 9 \text{ K}$  for water.

The experimental results are presented once more in Fig. 8 in the form of  $C = Nu_D/Ra_D^{1/4}$  vs.  $\alpha$  so as the very point in the Fig. 8 is now the average of the results for all cases shown in frames in Fig. 7. These points together with literature data [14–17] were approximated by the second-order spline curve (grey line) described mathematically by the expression placed in the lower frame. The black line of Fig. 8 is also the second-order spline

line but for the theoretical results, obtained by numerical evaluation of the integral (52).

As one can see the theoretical solution is convergent with experiments for vertical round plate  $\alpha = 0^\circ$  and for horizontal cone of the base angle  $\alpha \leq 60^\circ$ . For the cones of the base angle  $\alpha$  between  $60^\circ$  and  $90^\circ$  (horizontal cylinder) there is a divergences. It is a consequence of the use of the simplified asymptotic method of solution of Eq. (44).

The constants in Nusselt–Rayleigh experimental correlations recalculated for  $D$  as a characteristic linear dimension:  $C_{\text{exp}} = 0.749$  for  $\alpha = 30^\circ$ ,  $C_{\text{exp}} = 0.742$  for  $\alpha = 45^\circ$  and  $C_{\text{exp}} = 0.677$  for  $\alpha = 60^\circ$ , differs from the present solutions:  $C_{\text{theor}} = 0.746$  for  $\alpha = 30^\circ$ ,  $C_{\text{theor}} = 0.716$  for  $\alpha = 45^\circ$  and  $C_{\text{theor}} = 0.618$  for  $\alpha = 60^\circ$  of about:  $+0.4\%$  for  $\alpha = 30^\circ$ ,  $+3.5\%$  for  $\alpha = 45^\circ$  and  $-8.2\%$  and  $+8.7\%$  for  $\alpha = 60^\circ$ . This comparison can be regarded as a positive result of verification of obtained solution.

## 7. Conclusions

The results of the own experimental measurements and literature data of the free convective heat transfer in unlimited space of water and air from horizontal conics for the range of temperature differences  $9 \text{ K} \leq \Delta T \leq 43 \text{ K}$  for air and  $0.7 \text{ K} \leq \Delta T \leq 9 \text{ K}$  for water and Rayleigh numbers  $6 \times 10^5 < Ra < 2 \times 10^8$  for air and  $1 \times 10^7 < Ra < 2 \times 10^8$  for water are presented by the spline curve of the second-order for the base angle of the cone  $0 \leq \alpha \leq 90$  deg. The spline function has the form:  $C_{\text{exp}} = 0.672 + 3.959 \times 10^{-9}\alpha - 5.836 \times 10^{-5}\alpha^2$ .

The theory elaborated in this paper is based on the typical for natural convection assumptions and cover all conditions described above. The resulting differential equation of the theory (25) is one-dimensional in the coordinate system that was specially constructed to account the geometry of horizontal cones and the gravitational field.

The obtained approximate solution describes convective heat transfer over horizontal isothermal conic in unlimited space. The structure of boundary layer that define the heat transfer and streamlines near the conical surface is described by the Taylor series near the points at  $\epsilon = 0$ . In this paper we present the solution based only on the first three terms of series. The approximate method of solution of the differential equation for boundary layer thickness in principle does not allow to obtained the correct description of the thickness in the vicinity of the starting point  $\epsilon = -\epsilon_m$ . The consequence of this is the divergence of the integral (52) that define the mean value of heat transfer coefficient. For all the cases of conic angles  $\alpha$  we used universal approach of regularization of the integral.



Table 1  
Comparison of own and literature theoretical and experimental results of free convective heat transfer from horizontal cones

Case	Criterial relations	Notes
$\alpha = 0^\circ$ round vertical plate	$Nu = 0.763 \cdot Ra^{1/4}$	Present solution Experiment of vertical round plate of diameter $D = 0.07$ m, water, [14] Experiment of vertical round plate of diameter $D = 0.07$ m, air, [14] Numerical calculations, FLUENT/UNS program for round plate and air, [14]
	$Nu = 0.587 \cdot Ra^{1/4}$	
	$Nu = 0.655 \cdot Ra^{1/4}$	
	$Nu = 0.699 \cdot Ra^{1/4}$	
$\alpha = 30^\circ$	$Nu = 0.746 \cdot Ra^{1/4}$	Present solution Experiment in air for $D = 0.1$ m Experiment in water for $D = 0.1$ m Mean experimental correlation elaborated for air and water
	$Nu = 0.771 \cdot Ra^{1/4}$	
	$Nu = 0.727 \cdot Ra^{1/4}$	
	$Nu = 0.749 \cdot Ra^{1/4}$	
$\alpha = 45^\circ$	$Nu = 0.716 \cdot Ra^{1/4}$	Present solution Experiment in air for $D = 0.1$ m Experiment in water for $D = 0.1$ m Mean experimental correlation elaborated for air and water
	$Nu = 0.745 \cdot Ra^{1/4}$	
	$Nu = 0.738 \cdot Ra^{1/4}$	
	$Nu = 0.742 \cdot Ra^{1/4}$	
$\alpha = 60^\circ$	$Nu = 0.618 \cdot Ra^{1/4}$	Present solution Experiment in air for $D = 0.1$ m Experiment in water for $D = 0.1$ m Mean experimental correlation elaborated for air and water
	$Nu = 0.685 \cdot Ra^{1/4}$	
	$Nu = 0.669 \cdot Ra^{1/4}$	
	$Nu = 0.677 \cdot Ra^{1/4}$	
$\alpha = 90^\circ$ horizontal cylinder	$Nu = 0.480 \cdot Ra^{1/4}$	Experimental results of horizontal cylinders [15] Experimental results of horizontal cylinders [16,17] for $Pr \rightarrow \infty$ Experimental results of horizontal cylinders [16,17] for $Pr \rightarrow 0v$
	$Nu = 0.518 \cdot Ra^{1/4}$	
	$Nu = 0.599 \cdot Ra^{1/4}$	

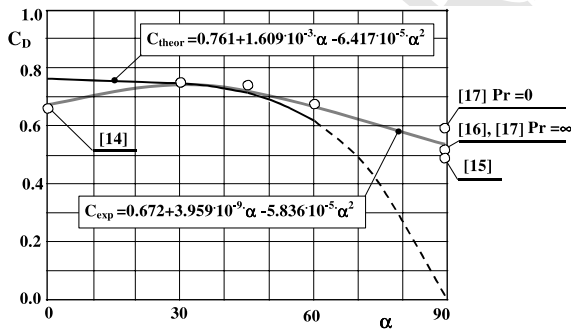


Fig. 8. Comparison of the own and literature experimental results described by  $C_D = Nu_D / Ra_D^{1/4}$  (points and gray line) with analytical solution (black line).

Eventually the discrepancy in the result of calculations is connected with this. We plan to improve this point of the theory by matching of two asymptomatic for both singular points  $\epsilon = 0$ ,  $\epsilon = -\epsilon_m$ . The algorithm described in the article allows to account arbitrary number of such terms in the Taylor series near the points at  $\epsilon = 0$  and hence improve the heat transfer description.

8. Uncited references 431

[12,13] 432

Acknowledgements 433

This research was supported by Scientific Research of the Chemistry Faculty Gdańsk University of Technology. 434 435

References 436

[1] Md. Alamgir, Over-all heat transfer from vertical cones in laminar free convection an approximate method, J. Heat Transfer Trans. ASME 101 (1979) 174–176. 437 438 439  
 [2] W.M. Lewandowski, S. Szymański, P. Kubski, E. Radziemska, H. Bieszk, Natural convective heat transfer from isothermal conic, Int. J. Heat Mass Transfer 42 (1999) 1895–1907. 440 441 442 443  
 [3] W.M. Lewandowski, P. Kubski, S. Szymański, H. Bieszk, T. Wilczewski, E. Radziemska, T. Seramak, Natural convective heat transfer from conical surfaces, in: V UK National Conference on Heat Transfer, 1997. 444 445 446 447

- 448 [4] W.E. Stewart, Asymptotic calculation of free convection in  
449 laminar three-dimensional systems, *Int. J. Heat Mass*  
450 *Transfer* 14 (1971) 1013–1031.
- 451 [5] R.G. Hering, Laminar free convection from non isother-  
452 mal cone at low Prandtl numbers, *Int. J. Heat Mass*  
453 *Transfer* 8 (1965) 1333–1337.
- 454 [6] P.H. Oosthuizen, E. Donaldson, Free convective heat  
455 transfer from vertical cones, *J. Heat Transfer Trans.*  
456 *ASME* (1972) 330–331.
- 457 [7] P.H. Oosthuizen, Free convective heat transfer from  
458 horizontal cones, *J. Heat Transfer Trans. ASME* (1973)  
459 409–410.
- 460 [8] S.W. Churchill, Free convection around immersed bodies,  
461 2.5 Single-Phase Convective Heat Transfer, in: 2.5 Single-  
462 Phase Convective Heat Transfer, Hemisphere Publishing  
463 Corporation, Washington, DC, 1983.
- 464 [9] S. Leble, W.M. Lewandowski, Analytical description of  
465 heat transfer by free convection from isothermal horizontal  
466 conic in unlimited space, *MPS: Applied Mathematics/*  
467 *0301006*.
- [10] S. Leble, W.M. Lewandowski, A theoretical consideration  
of a free convective boundary layer on an isothermal  
horizontal conic, *Appl. Math. Model.* (submitted).
- [11] W.M. Lewandowski, Natural convection heat transfer  
from plates of finite dimensions, *Int. J. Heat Mass Transfer*  
34 (3) (1991) 875–885.
- [12] H.B. Squire, in: S. Goldstein (Ed.), *Modern Developments*  
in *Fluid Dynamics*, Clarendon Press, Oxford, 1938, or in  
Dover, New York, 1965.
- [13] E.R.G. Eckert, *Heat and Mass Transfer*, McGraw-Hill  
Book Company, New York, 1959, pp. 312.
- [14] W.M. Lewandowski, E. Radziemska, Heat transfer by free  
convection from an isothermal vertical round plate in  
unlimited space, *Appl. Energy* 68 (2001) 187–201.
- [15] U.T. Morgan, The overall convective heat transfer from  
smooth circular cylinders, *Adv. Heat Transfer* 11 (1975)  
199–264.
- [16] S.W. Churchill, H.H.S. Chu, Correlating equations for  
laminar and turbulent free convection from a horizontal  
cylinder, *Int. J. Heat Mass Transfer* 18 (1975) 1049–1053.
- [17] B. Gebhart, Natural convection flows and stability, *Adv.*  
*Heat Transfer* 9 (1973) 273–346.

UNCORRECTED